

## Supplementary Materials and Methods

### Plasmids

A promoter/enhancer sequence (chr1: 28,292,241 – 28,293,179) of zebrafish (*Danio rerio*) *crystallin, alpha A* (*cryaa*) gene (*cryaa* promoter), that (chr5:9,071,149–9,075,275) of medaka (*Oryzias latipes*) *Sp7 transcription factor* (*sp7*) gene (*Ola.sp7* promoter), and that (chr6:45,506,296–45,506,852) of human (*Homo sapiens*) *runt related transcription factor 2* (*RUNX2*) gene (*Hsa.RUNX2* promoter) were obtained by the PCR amplification of species-specific genomic DNA, respectively (Knopf et al., 2011; Kurita et al., 2003; Spoorendonk et al., 2008). The medaka genomic DNA was kindly provided by H. Nishina (Tokyo Medical and Dental University, Japan). A promoter/enhancer sequence of *myosin, light chain 7, regulatory* (*myl7*) gene (*myl7* promoter) was described previously (Fukui et al., 2014).

Either full length or partial cDNA fragments encoding zebrafish *actinin, alpha 2* (*actn2*), *osteocrin* (*ostn*), *calcium-sensing receptor* (*casr*), *myogenic differentiation 1* (*myod1*), *sex determining region Y-box 9a* (*sox9a*), *runx2b*, *secreted phosphoprotein 1* (*spp1*), *collagen, type X, alpha 1* (*col10a1*), *natriuretic peptide receptor 2* (*npr2*), *natriuretic peptide receptor 3* (*npr3*), *natriuretic peptide C, like* (*nppcl*), mouse (*Mus musculus*) *Ostn* (*Mmu.Ostn*), and human *NPR3* (*Hsa.NPR3*) were amplified by PCR using species-specific cDNA libraries as templates and cloned into pCR4 Blunt TOPO vector (Thermo Fisher scientific). Primers used for cloning were listed in supplementary data (Table S1). cDNA fragments of zebrafish *connective tissue growth factor a* (*ctgfa*), *yes-associated protein 1* (*yap1*)-5SA, Yap1–Tead interfering peptide (*ytip*), *runx2a*, *sp7* and *Hsa. TEA domain transcription factor 2* (*TEAD2*) were described previously (Fukui et al., 2014; Kashiwada et al., 2015; Uemura et al., 2016). A cDNA fragment encoding a

yeast (*Saccharomyces cerevisiae*) GAL4-DNA-binding domain (*Gal4db*) fused to two transcriptional activation domains from VP16 (*GAL4FF*) was derived from a pCS2+Gal4FF vector.

To generate a pTol2-myl7 vector, a myl7 promoter was inserted into pTol2 vector, which was kindly provided by K. Kawakami (National Institute of Genetics, Japan) (Kawakami et al., 2004; Urasaki et al., 2006).

To construct a pTol2-myl7:actn2-tdEos plasmid, *EGFP* cDNA was removed from pEGFP-N1 vector (Clontech) and replaced with *tandem (td) Eos* cDNA derived from pcDNA3Flag-td-EosFP (Funakoshi) (ptdEos-N1 vector). A ptdEos-N1-actn2 plasmid was constructed by inserting *actn2* cDNA into the ptdEos-N1 vector. Finally, a cDNA fragment encoding *tdEos*-tagged *actn2* was subcloned into the pTol2-myl7 vector.

To construct a pTol2-myl7:ostn-HS4-hsp70l:EGFP plasmid, a chicken (*Gallus gallus*)  $\beta$ -globin insulator (*HS4*) derived from pJC13-1 vector, which was a gift from G. Felsenfeld (National Institute of Health, USA) (Chung et al., 1993) and a multiple cloning site (MCS) were sequentially subcloned into the pTol2-myl7: nuclear localization signal (NLS) tagged–monomeric (m) Cherry vector (Fukui et al., 2014) (pTol2-myl7:NLS-mCherry-HS4-MCS). A zebrafish heat shock protein (*hsp70l*) promoter followed by EGFP (*hsp70l:EGFP*) derived from pHSP70/4 EGFP plasmid (provided by J. Kuwada, University of Michigan, USA) (Halloran et al., 2000) were inserted into the pTol2-myl7:NLS-mCherry-HS4-MCS to generate pTol2-myl7:NLS-mCherry-HS4- hsp70l:EGFP. Finally, a *NLS-mCherry* cDNA fragment was removed and replaced with an *ostn* cDNA fragment.

To construct a pTol2-Ola.sp7:EGFP plasmid, a DNA fragment encoding *EGFP* and an Ola.sp7 promoter were sequentially inserted in to the pTol2 vector.

To construct a pTol2-Ola.sp7:GAL4FF-2A-mCherry plasmid, a cDNA fragment encoding *GAL4FF* followed by 2A peptide and *mCherry* (GAL4FF-2A-mCherry) and an Ola.sp7 promoter were sequentially inserted into the pTol2 vector. To construct a pTol2-Hsa.RUNX2:GAL4FF-2A-mCherry plasmid, a cDNA fragment encoding *GAL4FF-2A-mCherry* and a Hsa.RUNX2 promoter followed by a TATA box region of an adenovirus E1b minimal promoter derived from pFR-Luc (Stratagene) were sequentially inserted into the pTol2 vector. To construct a pTol2-Ola.sp7:Gal4db-Hsa.TEADΔN-2A-mCherry plasmid, a cDNA fragment encoding *Gal4db* was fused to *Hsa.TEAD2* cDNA lacking amino-terminus (1-113 a.a.) followed by 2A peptide and *mCherry* (Gal4db-Hsa.TEADΔN-2A-mCherry). Gal4db-Hsa.TEADΔN-2A-mCherry and Ola.sp7 promoter were sequentially inserted into the pTol2 vector.

To construct a pTol2-myl7:NLS-EGFP-HS4-UAS:EGFP-ytip, a DNA fragment encoding *NLS-mCherry* was removed from pTol2-myl7:NLS-mCherry-HS4-MCS vector and replaced with a cDNA fragment encoding *NLS-EGFP*. An upstream activating sequence (*UAS*) along with an E1b minimal promoter derived from pBluescript II-UAS:GFP vector was inserted to construct a pTol2-myl7:NLS-EGFP-HS4-UAS-MCS vector. Finally, a cDNA fragment encoding *ytip* was inserted into the pTol2-myl7:NLS-EGFP-HS4-UAS-MCS vector.

To construct a pTol2-cryaa:NLS-mCherry-HS4-UAS:EGFP-yap1-5SA plasmid, a myl7 promoter of a pTol2-myl7:NLS-mCherry-HS4-MCS vector was replaced by a cryaa promoter. A 5xUAS promoter derived from pTol2-5xUAS vector, a gift from K. Kawakami (National Institute of Genetics, Japan) (Asakawa et al., 2008; Distel et al., 2009), was subcloned to generate a pTol2-cryaa:NLS-mCherry-HS4-5xUAS-MCS vector. Finally, a cDNA fragment encoding *yap1-5SA* was inserted into the pTol2-

cryaa:NLS-mCherry-HS4-5xUAS-MCS vector. To construct a pEGFP-N1-Hsa.NPR3 plasmid, a *Hsa.NPR3* cDNA was inserted into the pEGFP-N1 vector. To construct a pCS3-npr2-EGFP plasmid, an *npr2* cDNA was inserted into the pEGFP-N1 vector. A cDNA fragment of *npr2-EGFP* was inserted into the pCS3 vector.

### Transgenic (Tg) fish lines and knockout fish by a transcription activator-like effector nuclease (TALEN) method

The transgenic fish lines; *Tg(myl7:actn2-tdEos)*, *Tg(myl7:ostn,hsp70l:EGFP)*, *Tg(Hsa.RUNX2:GAL4FF-2A-mCherry)*, *Tg(Ola.sp7:EGFP)*, *Tg(Ola.sp7:GAL4FF-2A-mCherry)*, *Tg(Ola.sp7:Gal4db-Hsa.TEAD2ΔN-2A-mCherry)*, and *Tg(myl7:NLS-EGFP,UAS:EGFP-ytip)* fish lines were established by injecting Tol2-based plasmids (30 pg) with transposase mRNAs (25 pg) into the one-cell stage of wild type strain AB zebrafish embryos (Kawakami et al., 2004; Urasaki et al., 2006). Embryos were selected at 2-5 days post-fertilization (dpf) and grown to adults, among which germline founders were identified by promoter specific fluorescence expression. *Tg(myl7:NLS-mCherry)* fish line was reported previously (Fukui et al., 2014).

TALEN sequence against the second exon of *ostn* was designed using TAL Effector Nucleotide Targeter (Doyle et al., 2012). The *ostn* TALEN was generated using Golden Gate TALEN and TAL Effector Kit 2.0 (Addgene) (Cermak et al., 2011). The *ostn* TALEN recognition sequences are: 5'-TCTTGTCTGCTGACACTGACC-3' and 5'-CCGAAAGCCTTCACATA-3'. The sequence between the two binding sites contains a 16-bp spacer with a PstI site (TTGTTCCACTGCAGTG, PstI site underlined). TALEN mRNAs were *in vitro* transcribed from SacI-linearized expression plasmids with T3 RNA polymerase using a mMESSAGE mRNA kit (Ambion). A total of 200 pg TALEN mRNAs was microinjected into one-cell stage embryos. Mutant alleles were identified

by PstI digestion of a PCR product generated with the primers listed in the supplemental information (Table S1).

### Chemicals, peptides, and antibodies

KT5823 was purchased from Calbiochem; synthetic human C-type natriuretic peptide (CNP) -22 from Peptide Institute; anti-YAP1/WWTR1 antibody (63.7) from Santa Cruz, Alexa Fluor 488-labeled secondary antibody and 4', 6-diamidino-2-phenylindole, dihydrochloride (DAPI) from Thermo Fisher Scientific; Streptavidin Cy3 conjugate, insulin, and 3-isobutyl-1-methylxanthine (IBMX) were from Sigma-Aldrich. Mouse osteocrin (OSTN) (80-130 a.a.), rat (*Rattus norvegicus*) OSTN (82-132 a.a.), and biotin-labeled rat OSTN (82-132 a.a.) were synthesized by Sigma-Aldrich.

### Microinjection of oligonucleotide and mRNA

For morpholino oligonucleotide (MO)-mediated gene knock down, embryos were injected at the one-cell stage with 4-10 ng of Control MO (Gene Tools), 8-15 ng of *ostn* splicing block MO (5'-CATTCTTTATTTCACTACCTCTGC-3'), 3-5 ng of *npr2* splicing block MO (5'-AACCAAGAACTCAACTCACCCCA-3'), and 4 ng of translation block *ctgfa* MO (5'-GAGTCATTCCAGAAAACATGATGAC -3'). The sequence of *ctgfa* MO has already been validated (Fukui et al., 2014).

Capped mRNAs were *in vitro* transcribed with SP6 RNA polymerase using a mMESSAGE mMACHINE kit (Ambion). For protein overexpression, one-cell stage embryos were injected with 100 pg of *EGFP* mRNA or 100 pg of *ctgfa* mRNA. For rescue experiment, one-cell stage embryos were coinjected with 4 ng of *npr2* MO and 160 pg of *npr2-EGFP* mRNA.

For EGFP-Yap1-5SA expression, one-cell stage of *Tg(Ola.sp7:GAL4FF-2A-mCherry)* embryos were injected with 30 pg of pTol2-cryaa-NLS-mcherry-HS4-5xUAS-EGFP-yap1-5SA plasmid. As a negative control, embryos were injected with 30 pg of pTol2-cryaa-NLS-mCherry-HS4-5xUAS-MCS plasmid and mCherry-positive embryos were selected for the experiment.

### Fluorescence-activated cell sorting (FACS)

Hearts resected from the *Tg(myl7:NLS-mCherry)* or *Tg(myl7:actn2-tdEos)* larvae at 72 hours post-fertilization (hpf) were collected into a 1.5 ml tube, washed in phosphate buffered saline (PBS), and incubated with 1 ml of protease solution (PBS with 5 mg/ml trypsin and 1 mM EDTA, pH 8.0) for 1 h under occasional pipetting. Digestion of the hearts were terminated with 200 µl of stop solution (PBS with 30% fetal bovine serum [FBS] and 6 mM calcium chloride). The dissociated cells in suspension medium (phenol red free Dulbecco's modified Eagle's medium [DMEM, Life Technologies] with 1% FBS, 0.8 mM calcium chloride, 50 U/ml penicillin, and 0.05 mg/ml streptomycin) were subjected to cell sorting using a FACS Aria III cell sorter (BD Bioscience). mCherry- or tdEos-positive cells were collected as cardiomyocytes for further RNA preparation.

### RNA preparation, RNA sequence (RNA-seq), and quantitative (q) RT-PCR

For RNA-seq, total RNAs were prepared from mCherry- or tdEos-positive cells using a NucleoSpin XS kit (Macherey-Nagel) according to the manufacture's instruction. Reverse transcription (RT) and cDNA library preparation were performed with a SMARTer Ultra Low RNA kit (Clontech). cDNA was fragmented with a Covaris S 220 instrument (Covaris). Subsequently, the sample was end-repaired, dA-tailed, adaptor ligated, and then subjected to PCR by using a NEBNext DNA Library Preparation and

NEBNext Multiplex oligos for Illumina (New England BioLabs). The sample was sequenced by using a MiSeq (Illumina) to generate pair-end 150-bp reads. Raw reads were mapped to zebrafish genome (DanRer7). Expression levels were measured by calculating reads per kilobase per million sequenced reads (RPKM) and normalized trimmed mean of M-values (TMM) method using an Avadis NGS software (Strand Life Sciences).

For RT-PCR, total RNAs were prepared from zebrafish larvae, mouse organs, or MC3T3-E1 cells using TRIzol reagent (Thermo Fisher Scientific). RNAs were reverse-transcribed by random hexamer primers using SuperScript III (Thermo Fisher Scientific) according to the manufacturer's instructions. PCR reactions was performed with TaKaRa Ex Taq Hot Start Version (TaKaRa) in a 2720 Thermal Cycler (Thermo Fisher Scientific). For qRT-PCR, PCR reactions were performed with KOD SYBR qPCR Mix (TOYOBO) in a Mastercycler Realplex (Eppendorf). The primers used for RT-PCR and qRT-PCR were listed in supplementary data (Table S1).

### **Whole mount *in situ* hybridization (WISH)**

Antisense *ostn*, *casr*, *myl7*, *myod1*, *sp7*, *sox9a*, *runx2a*, *runx2b*, *spp1*, *coll10a1*, *npr2*, *npr3*, *nppcl*, and *ctgfa* RNA probes labeled with digoxigenin (DIG) were *in vitro* transcribed using an RNA labeling kit (Roche). WISH was performed according to the standard protocol as described previously (Fukui et al., 2014). Briefly, embryos and larvae were fixed in 4% paraformaldehyde (PFA) in PBS, dehydrated in methanol (MeOH), and gradually rehydrated into PBS containing 0.1% Tween 20 (PBS-T). For parasphenoid (ps) observation, larvae were resected the lower jaws. After digestion by PBS-T containing proteinase K (Roche) for 15-50 min, embryos and larvae were fixed

in 4% PFA and hybridized with antisense RNA probes at 65°C (*ostn*, *casr*, *myl7*, and *myod1* probes) or 70°C (the others) overnight in hybridization buffer (5 x SSC, 50% formamide, 5 mM EDTA, 0.1% tween20, 50 µg/ml heparin, and 1 mg/ml torula RNA). After hybridization, embryos and larvae were incubated with anti-DIG antibody conjugated with alkaline phosphatase (Roche) in blocking buffer at 4°C overnight. The colorimetric reaction was carried out using BM purple (Roche). Images of the embryos were recorded with a SZX16 Stereo microscope (Olympus).

### Plastic section for ISH

Larvae hybridized with antisense *ostn*, *myod1*, *sp7*, and *sox9a* probe were dehydrate with acetone, embedded in Technovit 8100 (Heraeus Kulzer), and cut into 10 µm thick sections with a microtome (RM2125RT, Leica). Images of the sections were recorded with a BX51 microscope (Olympus).

### Bone staining

Larvae at 5-10 dpf were fixed in PBS containing 4% PFA at 4°C overnight and stored in 100% MeOH at -20°C. For alizarin red staining, larvae were gradually rehydrated into water, bleached in 1.5% hydrogen peroxide in 1% potassium hydroxide (KOH) for 30 min, and washed in water. The bones were stained with 0.04 mg/ml Alizarin Red S in 1% KOH, destained with 20% glycerol in 1% KOH for 1 h, and stored in 50% glycerol in 0.25% KOH. For alcian blue staining, larvae were stained with 0.02% Alcian Blue 8GX in 70% ethanol (EtOH) containing 80 mM magnesium chloride (MgCl<sub>2</sub>) at room temperature (RT) overnight, rehydrated into water, bleached in 1.5% hydrogen peroxide in 1% KOH for 30 min, and stored in 50% glycerol in 0.25% KOH. Cartilages were



dissected out, mounted in glycerol on slide glasses, and covered with cover slips. Bone images were recorded with a SZX16 Stereo microscope (Olympus) and the bone length was measured by a DP2-BSW software (Olympus). To detect the chondrocyte area, each chondrocyte was demarcated by drawing lines in the middle of cell border and measured the area inside of the lines.

To visualize live mineralized bone, larvae were incubated in 0.003% Alizarin red in 0.03% sea salt for 1 h. Confocal images were taken with a FV1000 confocal microscope system (Olympus) and the bone length was measured by Imaris software (Bitplane).

### **Measurement of head length**

Embryos and larvae at 2-6 dpf were fixed in PBS containing 4% PFA at 4°C overnight, washed in PBS, and mounted in glycerol. Images were recorded with a SZX16 Stereo microscope (Olympus). The head length was measured by a DP2-BSW software (Olympus).

### **5-Ethynyl-2-deoxyuridine (EdU) assay**

Larvae at 5 dpf were incubated in 200  $\mu$ M EdU (Tokyo Chemical Industry). After 24 h incubation, larvae were fixed in 4% PFA at 4°C overnight and dehydrated with MeOH. Larvae were rehydrated into PBS-T, resected their brain by forceps, permeabilized by 0.5% triton X-100, blocked with 3% bovine serum albumin (BSA) at RT for 30 min, and stained with Click-iT EdU Alexa Fluor 647 Imaging Kit (Thermo Fisher Scientific) for 30 min. The quantification of EdU-positive cells were performed by using the images of the stained sections observed by a FV1000 confocal microscope (Olympus) and analyzed by IMARIS7.7.1 software (Bitplane).

### **TdT-mediated dUTP nick end labeling (TUNEL) assay**

Larvae at 6 dpf were fixed in 4% PFA at 4°C overnight and dehydrated with MeOH. Larvae were rehydrated into PBS-T, resected the brain by forceps, digested by PBS-T containing proteinase K for 50 min at RT, and fixed in 4% PFA for 20 min at RT. After three times washing with PBS-T, larva were incubated with In Situ Cell Death Detection Kit, TMR red (Roche) for 60 min at 37°C. The quantification of TUNEL-positive cells were performed by using the images of the stained sections observed by a FV1000 confocal microscope (Olympus) and analyzed by IMARIS7.7.1 software (Bitplane).

### **Cell Culture, transfection, and siRNA-mediated knockdown**

Murine MC3T3-E1 osteoblast-like cells were obtained from Riken BRC and cultured in minimum essential medium  $\alpha$  (MEM $\alpha$ , Thermo Fisher Scientific) with 10% FBS and antibiotics (100 mg/ml streptomycin and 100 U/ml penicillin). Human embryonic kidney HEK293T cells and Murine NIH3T3 fibroblast cells were cultured in DMEM (Nacalai Tesque) with 10% FBS and antibiotics. Murine ATDC5 chondrocyte cells were obtained from Riken BRC and cultured in a 1:1 mixture of DMEM and Ham's F-12 Nutrient Mixture (Nacalai Tesque) (DMEM/F12) with 5% FBS. HEK293T cells transfected with plasmids using polyethylenimine (PEI) max (Polyscience) were subjected to binding assay. MC3T3-E1 cells transfected with siRNAs from Thermo Fisher Scientific (listed in supplementary Table S2) using Lipofectamine RNAi MAX reagents (Thermo Fisher Scientific) were subjected to immunocytochemical analyses.

## OSTN binding assay

Streptavidin conjugated Cy3 was diluted ten times and incubated with biotin, rat OSTN, or biotin-labeled rat OSTN on ice for 15 min to form OSTN-B–SA–Cy3. HEK293T cells transfected with pEGFP-N1–NPR3 or pEGFP-C1 empty vector (Clontech) and MC3T3–E1 cells were cultured for more than 24 h. HEK293T cells detached by pipetting using PBS and MC3T3–E1 cells treated by trypsin were resuspended with DMEM containing 10% FBS at  $2 \times 10^6$  cells/ml. After the incubation of cells with either CNP or unlabeled rat OSTN for 5 min, 0.1  $\mu$ M OSTN-B–SA–Cy3 was added into the mixture and incubated for 30 min. The cells were washed with 15 ml PBS and resuspended in PBS containing 1% BSA, 0.2 mg/ml sodium azide, and SYTOX Blue Dead Cell Stain (Thermo Fisher Scientific). Cy3 and EGFP fluorescence intensities were measured by FACS Aria III cell sorter (BD Bioscience). The data was analyzed using FACSDiva software (BD Bioscience).

## Immunocytochemical analyses

MC3T3–E1 cells or ATDC5 cells were plated in 35-mm glass-base dishes (Asahi Techno Glass) coated with 1% gelatin. To examine the localization of YAP1/WWTR1, the cells were stimulated with human CNP for the time indicated in the figures in the presence or absence of mouse OSTN with or without a protein kinase G (PKG) inhibitor. After stimulation, the cells were fixed in PBS containing 4% PFA at RT for 15 min, permeabilized with 0.2% Triton X-100 at RT for 10 min, and blocked with PBS containing 3% BSA at RT for 1 h. The cells were immunostained with anti-YAP/WWTR1 antibody at RT for 2 h and visualized using Alexa Fluor 488-labeled secondary antibody. DAPI was used to counterstain nuclei. Fluorescence images of Alexa 488 and DAPI were recorded with a confocal microscope (FV1000, Olympus)

with 40x water objective lens (LUMPlanFL, FN 26.5, Olympus).

### **Measurements of intracellular cGMP**

MC3T3-E1 cells, grown in 24 well plates, were incubated with incubation medium (DMEM containing 0.1% BSA and 500  $\mu$ M IBMX) at 37°C for 30 min. The cells were subsequently stimulated with incubation medium containing 0.1-100  $\mu$ M human CNP at 37°C for 15 min, replaced with ice cold 70% EtOH, and stored at -80°C. Cell lysates were transferred to test tubes, concentrated using a speedvac concentrator (Thermo scientific), and resuspended in 25  $\mu$ l of double distilled water. The amount of cGMP in each cell lysate was measured using a cyclic GMP radioimmunoassay kit (Yamasa) according to the manufacturer's protocol.

### **Light sheet imaging**

To record fluorescence in the beating heart, we used a lightsheet microscope (Lightsheet Z.1, Carl Zeiss). Larvae were anesthetized in 0.016% tricaine in 0.03% sea salt and transferred into 50  $\mu$ l glass capillaries with 1% low-melting agarose dissolved in 0.03% sea salt. Images were processed with a ZEN2012 software (Carl Zeiss).

### **Bright field movie**

To record bright field movies of larvae heart beating of, we used a SZX16 Stereo microscope (Olympus). Images were processed with a DP2-BSW software (Olympus).

# Supplementary table S1. Primers used for genotyping, cassette amplification, RT-PCR, and qRT-PCR.

Primer Name	Sequence (5'-3')
For genotyping	
ostn-gTAL-fw	ATGCTGGGCTGTGGATGTGTGCT
ostn-gTAL-rev	CAGAGGCTCTCTAGGGGAAA
For RT-PCR and qPT-PCR	
<i>ostn</i> (Dr)-fw	CTGACACTGACCTTGTTCCACT
<i>ostn</i> (Dr)-rev	TACACCAATCCGGTCAATCG
<i>eef1a111</i> (Dr)-fw	AACCCCAAGGCTCTCAAATC
<i>eef1a111</i> (Dr)-rev	GCACAGCAAAGCGACCAAG
<i>npr2</i> (Dr)-fw	GACAGCCCTGAGTATACCGC
<i>npr2</i> (Dr)-rev	TGCACGGAGAGAATCCACAG
<i>sp7</i> (Dr)-fw	TCCAGACCTCCAGTGTTTCC
<i>sp7</i> (Dr)-rev	ATGGACATCCCACCAAGAAG
<i>col10a1</i> (Dr)-fw (+77)	AGAAGGTGATGAAGGCCCGCAGTAC
<i>col10a1</i> (Dr)-rev (+217)	CACCATCTTGTCCTGCAGGTCCAGGT
<i>Ctgf</i> (Mm)-fw	ATTTGGCCCAGACCCAACTA
<i>Ctgf</i> (Mm)-rev	GGCTCTGCTTCTCAGtCTG
<i>Npr2</i> (Mm)-fw	TTTCCGGAAGCTGATGCTG
<i>Npr2</i> (Mm)-rev	TGACCGGTGTTGGCAAAGAT
<i>Npr3</i> (Mm)-fw	GAAGTACTCAGAGCTGGCTACAGCA
<i>Npr3</i> (Mm)-rev	CCTGCTTCAGTGTCAGTCATGGCAA
<i>Actb</i> (Mm)-fw	GTGACGTTGACATCCGTAAAGA
<i>Actb</i> (Mm)-rev	GCCGGACTCATCGTACTCC
For Cloning	
XhoI- <i>actn2</i> (Dr)-fw	CTCGAGATGATGAATCAGATCGAGCTTTCAGT GCCT
Asp718- <i>actn2</i> (Dr)-rev	GGTACCGTAAGGTCACTTTCTCCATATAGGGC

	GGTGGAG
PacI- <i>ostn</i> (Dr)-fw	TTAATTAACAGATTAAGGATGCTGGGCTGTGG
	AT
PacI- <i>ostn</i> (Dr)-rev	TTAATTAAACCTGCAATATTCCCCTGTATTTGC
	C
BamHI- <i>casr</i> (Dr)-fw	GGATCCTGGGTCTTTTCTACATCCCTCAGA
<i>casr</i> (Dr)-rev	GTCTTTAAAGCCGGGTATATGTCC
BamHI- <i>myod1</i> (Dr)-fw	GGATCCAAGATGGAGTTGTCTGGATATCC
<i>myod1</i> (Dr)-rev	AGAATTTTAAAGCACTTGATAAATGG
<i>Sox9a</i> (Dr)-fw	GCGAGCTGAGCAGCGATGTT
<i>Sox9a</i> (Dr)-rev	GCATGCAAATTAAGTAGAAC
BamHI- <i>spp1</i> (Dr)-fw	GGATCCGGACCAGGCAGCTACAGAAG
<i>spp1</i> (Dr)-rev	CACTGCCGTCTGTCGTCTAA
BamHI- <i>npr2</i> (Dr)-fw	GGATCCATTGTGCTGCTTACACGCATGGTCG
<i>npr2</i> (Dr)-rev	CATTCCACTGGATATCTGAACCCTG
BamHI- <i>npr2</i> (Dr)-fw (-14)	GGGATCCTTTGCCAACATAAGATGGGATCGCT
<i>npr2</i> (Dr)-rev (+1652)	GCCACCAGGTTGCCCTTAAAATAGC
<i>npr2</i> (Dr)-fw (+1526)	ATCACAAGCGTGCAGGAAGCC
NheI- <i>npr2</i> (Dr)-rev (+1652)	GCTAGCCCTGGCATCAACAGTGCTCTCA
<i>npr3</i> (Dr)-fw	ATGTCATGTTTCATGCCACTCTGTCTGTCC
<i>npr3</i> (Dr)-rev	CTACGCTGCTGAAAAGTTGGATCTGATGGA
BamHI- <i>nppcl</i> (Dr)-fw	GGATCCCTGACCCAGAATCAGCATCTCCA
<i>nppcl</i> (Dr)-rev	ATCCGCACTCGATGACGTCTGTG
<i>sp7</i> (Dr)-fw	TTAGACATGACGCATCCTTACG
<i>sp7</i> (Dr)-rev	CGTTGCCTGTGCTGCTCTTTTC
<i>runx2a</i> (Dr)-fw	CCACGCCGAACCTCCTTCAATC
<i>runx2a</i> (Dr)-rev	TCAATATGGCCGCCACACGGA

<i>runx2b</i> (Dr)-fw	ATGCGCATTCCCGTAGATCC
<i>runx2b</i> (Dr)-rev	TCAATACGGCCTCCAAACGCC
<i>col10a1</i> (Dr)-fw (+1326)	TGGCCCAGCAGGTCCTGGAGGCCCA
<i>col10a1</i> (Dr)-rev (+1772)	TTATAAAGTGCCACTAAAGCATTAG
SallI- <i>Ostn</i> (Mm)-fw	GTCGACATGCTGGACTGGAGATTGGCA
NotI- <i>Ostn</i> (Mm)-rev	GCGGCCGCTCAGCCTCTGGAAGTGGAGAGCC GGTT
NheI- <i>NPR3</i> (Hs)-fw	GCTAGCATGCCGTCTCTGCTGGTGCTCACTTT CTCC
BamHI- <i>NPR3</i> (Hs)-rev	GGATCCCGAGCTACTGAAAAATGGGATCTGAT GGAATC

---

**Supplementary table S2. siRNAs used for knockdown.**


---

siRNA Name	Sequence (5'-3')
NPR2#1	TAGCACTTCGAAGTGGTCCTTTCTA
NPR2#2	CAGCCCATGGGAAATACCAGATCTT

---

## Supplementary Figures

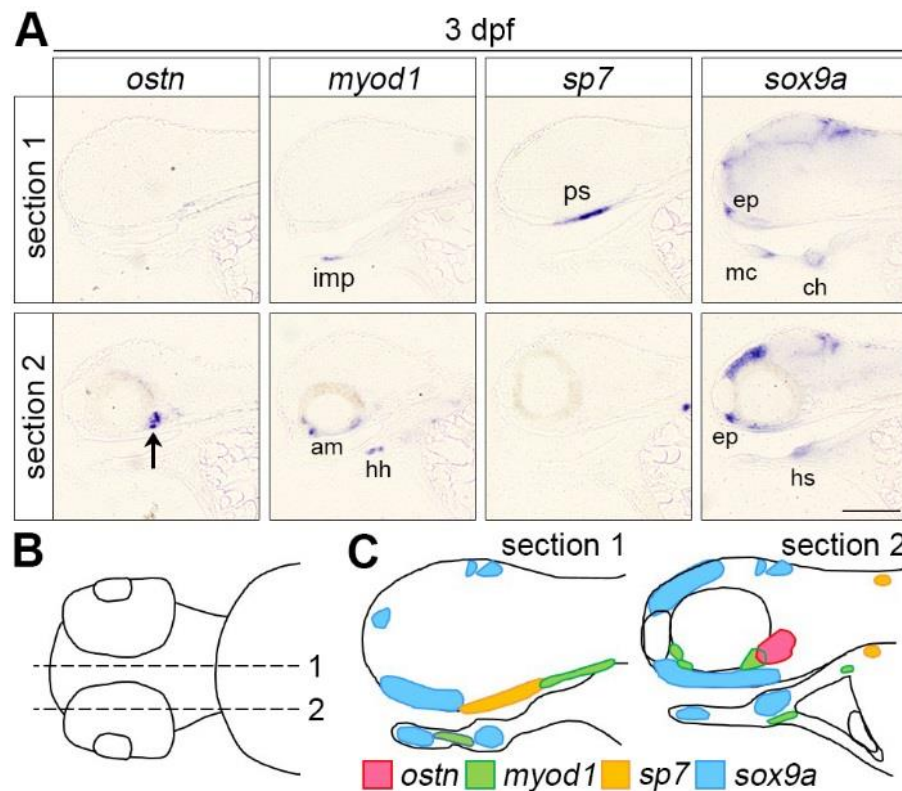


**Fig. S1. *osteocrin* (*ostn*) mRNA in the head.** (A) Whole mount *in situ* hybridization (WISH) analyses of mRNAs indicated at the top in the larvae at 3 days post-fertilization (dpf). Sagittal sections of midline (upper panels, section 1) and the *ostn* expressing area (lower panels, section 2), anterior to the left. The arrow indicates *ostn* mRNA expression. imp, intermandibularis posterior; am, adductor mandibulae; hh, hyohyoideus; ps, parasphenoid; ep, ethmoid plate; mc, meckel's cartilage; ch, ceratohyal; hs, hyosymplectic. Scale bar, 100  $\mu$ m. (B) Schematic drawing of the zebrafish head at 3 dpf, ventral view, anterior to the left. Broken lines indicate the planes of section 1 (upper line) and section 2 (lower line). (C) Schematic drawing of the expression of mRNAs indicated at the bottom. Section 1 (left) and section 2 (right), anterior to the left.



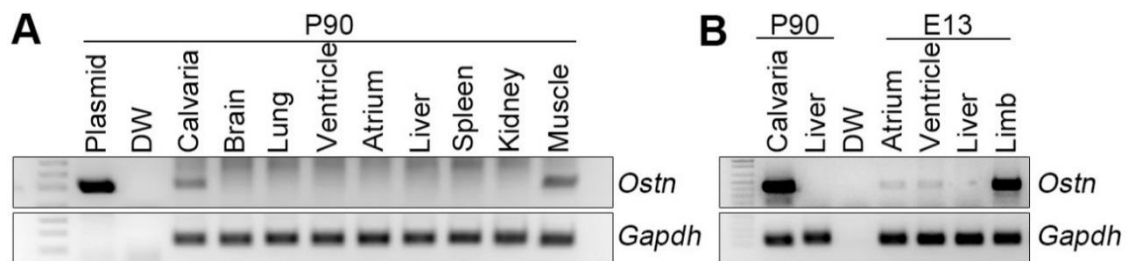


**Fig. S2. *ostn* mRNA expression in the mouse organs.** (A) Representative results of reverse transcription (RT)-PCR analyses of *Ostn* (upper panel) and *Gapdh* (lower panel) mRNAs in postnatal day 90 (P90) mouse organs indicated at the top. pCR4-Mmu.Ostn (Plasmid) and distilled water (DW) were used as a positive and a negative control, respectively. (B) RT-PCR analyses of embryonic day 13 (E13) mouse organs indicated at the top. P90 mouse organs and DW were used as controls.

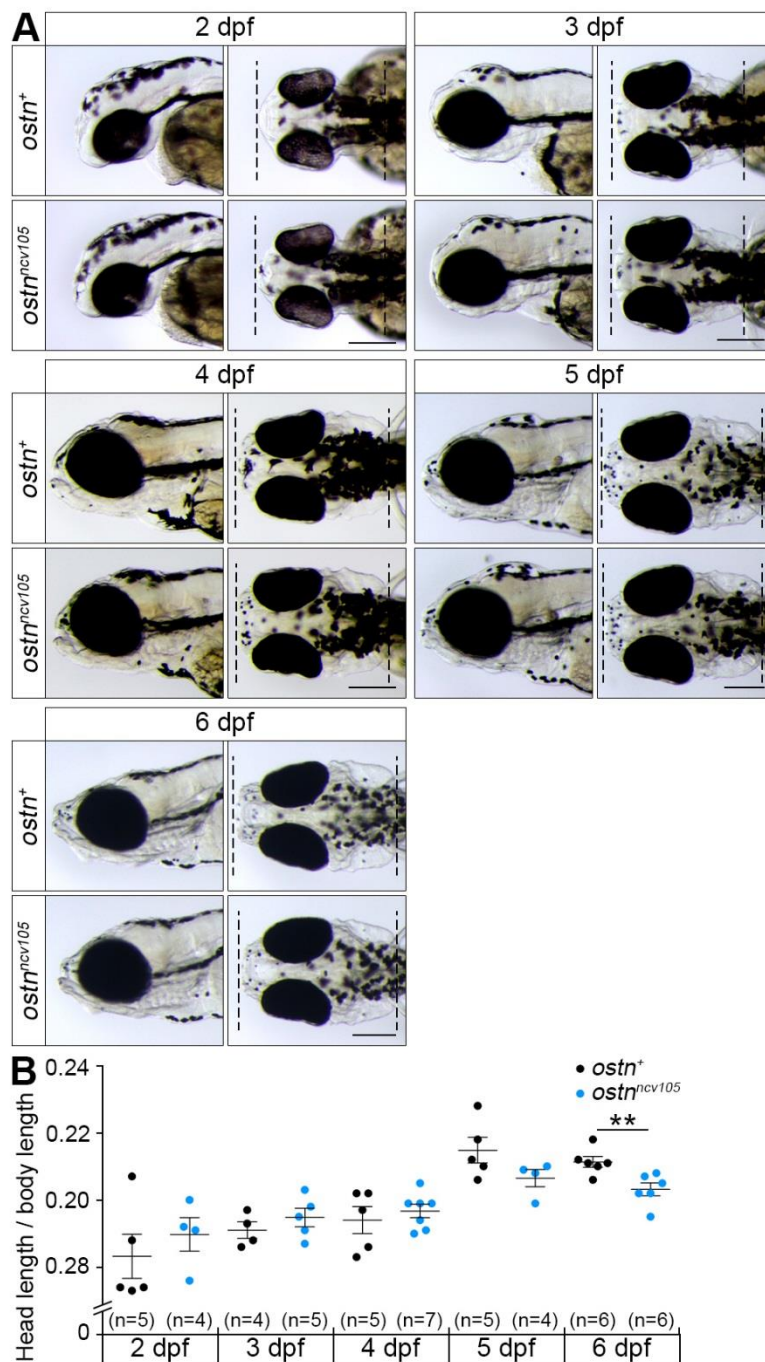


**Fig. S3. Head morphology and length of *ostn* mutants.** (A) Representative images of the head of the 2-6 dpf wild type (upper panels) and homozygous mutant (lower panels) embryos and larvae. Lateral view (left panels) and dorsal view (right panels), anterior to the left. Broken lines indicate the tip and the end of the heads. (B) The ratio of the head length (from the tip of the head to the center of hourglass like shape at the back of the head) to the body length (from the tip of the upper jaw to the end of the tail) of wild type (*ostn*<sup>+</sup>) or homozygous mutant (*ostn*<sup>ncv105</sup>) larvae at 2-6 dpf. The data were analyzed by Student's *t*-test. Statistical significance, \*\**p* < 0.01. Error bars indicate s.e.m. Scale bars, 200  $\mu$ m.

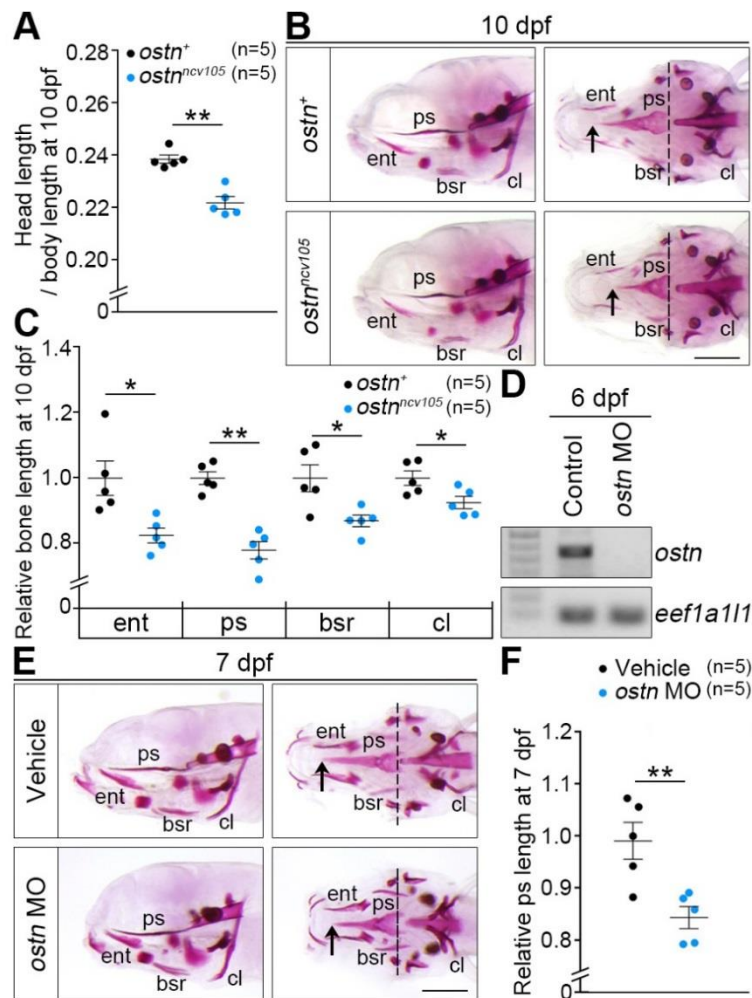


**Fig. S4. Depletion of Ostin results in shortening of the ps and other intracranial membranous bones.** (A) The ratio of the head length to the body length of the 10 dpf wild type (*ostn*<sup>+</sup>) or homozygous mutant (*ostn*<sup>ncv105</sup>) larvae was analyzed similarly to Fig. 3C. (B) Representative images of alizarin red staining of the 10 dpf larvae of wild type (upper panels) and homozygous mutant (lower panels). Lateral view (left panels) and ventral view (right panels), anterior to the left. Arrows and broken lines indicate the tip and the top of the concave in the caudal part of the parasphenoid, respectively. ent, entopterygoid; ps, parasphenoid; bsr, branchiostegal ray; cl, cleithrum. (C) Quantitative analyses of (B). Each relative bone length to the mean length of wild type bones was plotted. The length of ps was measured similarly to Fig. 3E. (D) A representative result of RT-PCR analyses of *ostn* (upper panel) and *eef1a111* (lower panel) mRNAs of the larvae injected with control morpholino oligonucleotide (MO) and *ostn* MO at 6 dpf. (E) Representative images of alizarin red staining of the 7 dpf larvae injected with vehicle (upper panels) and *ostn* MO (lower panels). Lateral view (left panels) and ventral view (right panels), anterior to the left. (F) Quantitative analyses of (E). The data were analyzed by Student's *t*-test. Statistical significance, \**p* < 0.05; \*\**p* < 0.01. Error bars indicate s.e.m. Scale bars, 200  $\mu$ m.

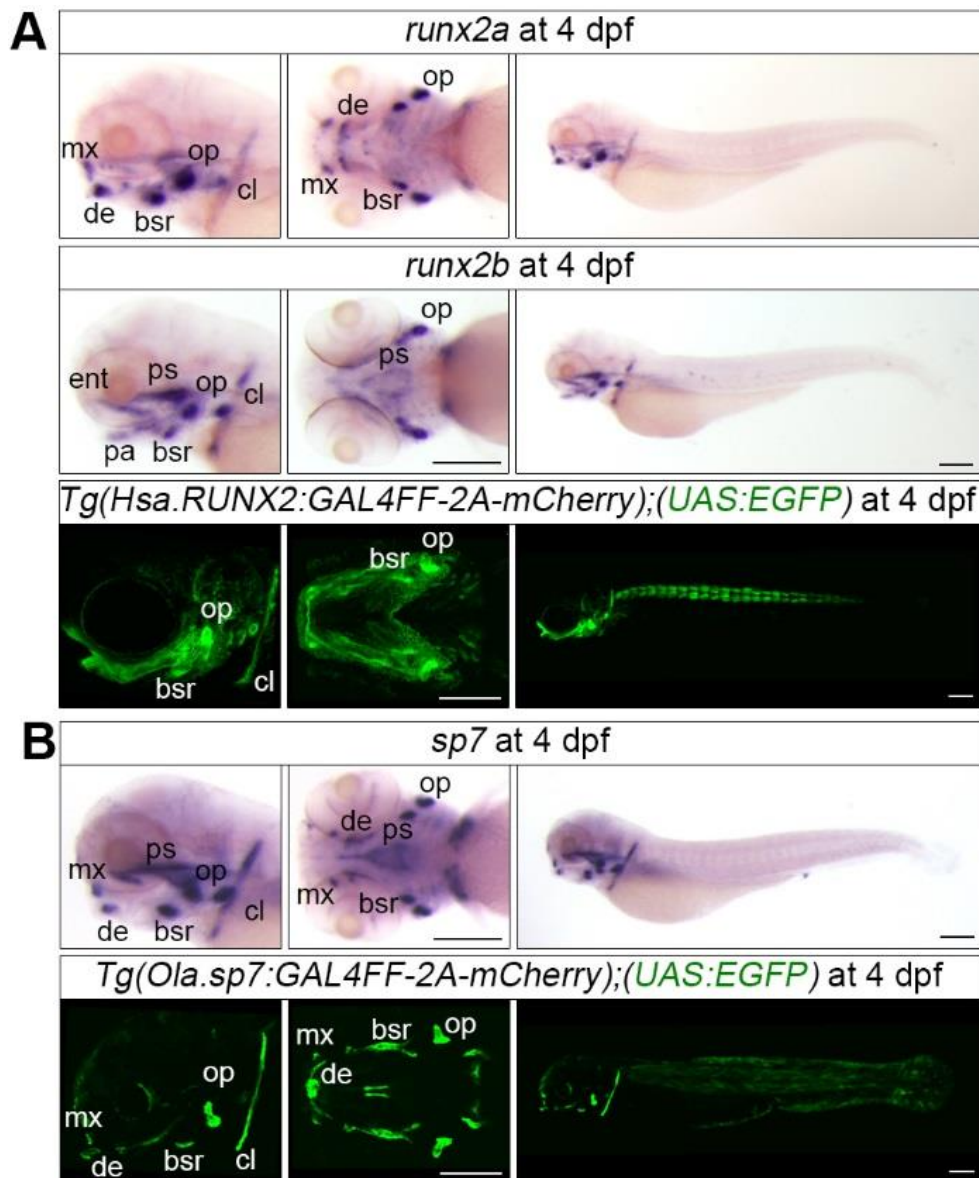


**Fig. S5. The EGFP reporter expression reflects endogenous *runx2a/b* and *sp7* mRNA expression.** (A) WISH analyses of *runx2a* (upper panels) and *runx2b* mRNAs (middle panels) in the larvae at 4 dpf. Projection views of confocal images of EGFP reporter expression in a *Tg(Hsa.RUNX2:GAL4FF-2A-mCherry);(UAS:EGFP)* (bottom panels) larva at 4 dpf. Lateral view of the head (left panels), ventral view of the head (center panels), and lateral view of the whole body (right panels), anterior to the left. (B) WISH analysis of *sp7* mRNA expression (upper panels) in a larva at 4 dpf. Projection views of confocal images of EGFP reporter expression in a *Tg(Ola.sp7:GAL4FF-2A-mCherry);(UAS:EGFP)* (bottom panels) larva at 4 dpf. Lateral view of the head (left panels), ventral view of the head (center panels), and lateral view of the whole body (right panels), anterior to the left. mx, maxilla; de, dentary; pa, pharyngeal arches; ent, entopterygoid; ps, parasphenoid; bsr, branchiostegal ray; op, opercle; cl, cleithrum. Scale bars, 200  $\mu$ m.



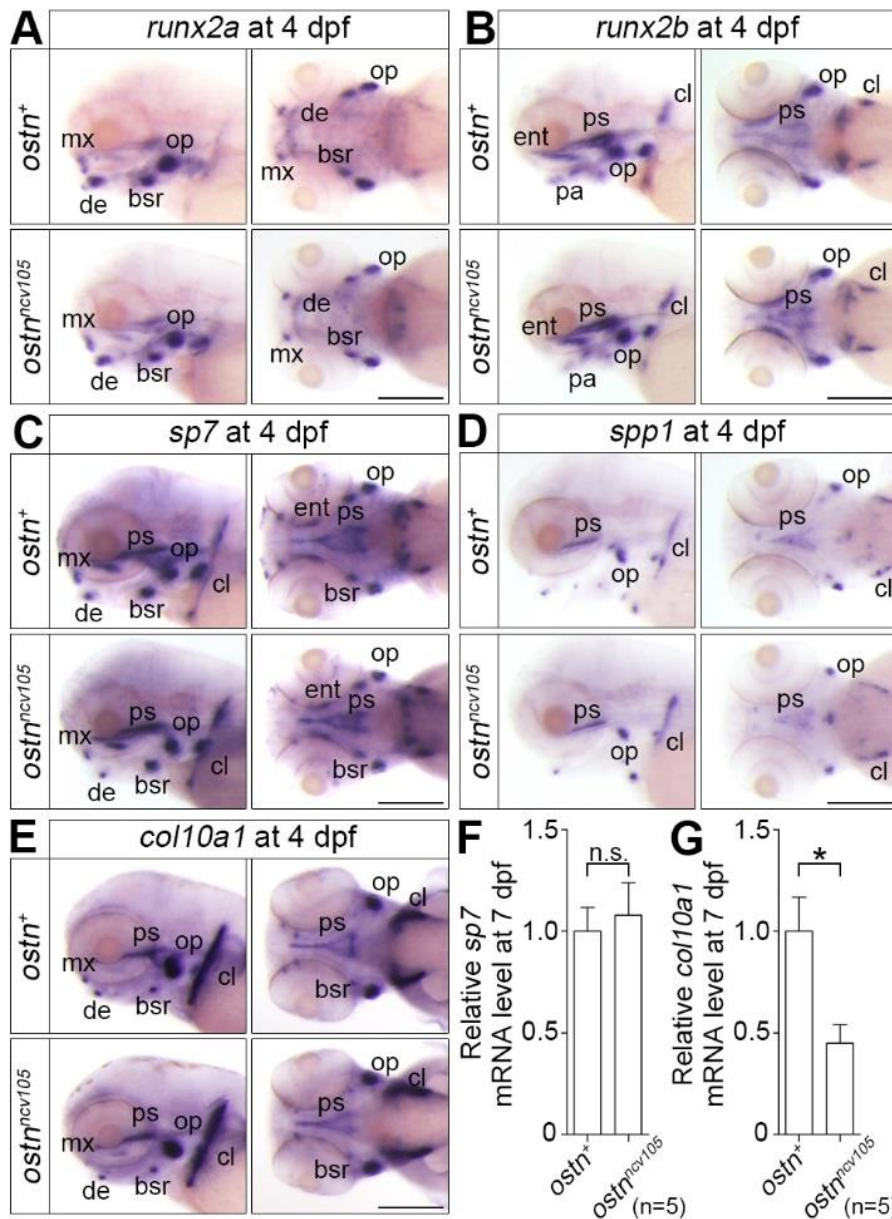


**Fig. S6. ECM expression was reduced in *ostn* mutant.** (A-E) WISH analyses of *runx2a* (A), *runx2b* (B), *sp7* (C), *spp1* (D), and *col10a1* mRNAs (E) in the 4 dpf larvae of wild type (upper panels) and *ostn*<sup>ncv105</sup> mutant (lower panels). Lateral view (left panels) and dorsal view (right panels), anterior to the left. mx, maxilla; de, dentary; pa, pharyngeal arches; ent, entopterygoid; ps, parasphenoid; bsr, branchiostegal ray; op, opercle; cl, cleithrum. (F, G) qRT-PCR analyses of *sp7* (F) and *col10a1* (G) mRNAs of wild type (*ostn*<sup>+</sup>) or homozygous mutant (*ostn*<sup>ncv105</sup>) larvae at 7 dpf. The data were analyzed by Student's *t*-test. Statistical significance, \**p* < 0.05; n.s., no significance between two groups. Error bars indicate s.e.m. Scale bars, 200  $\mu$ m.

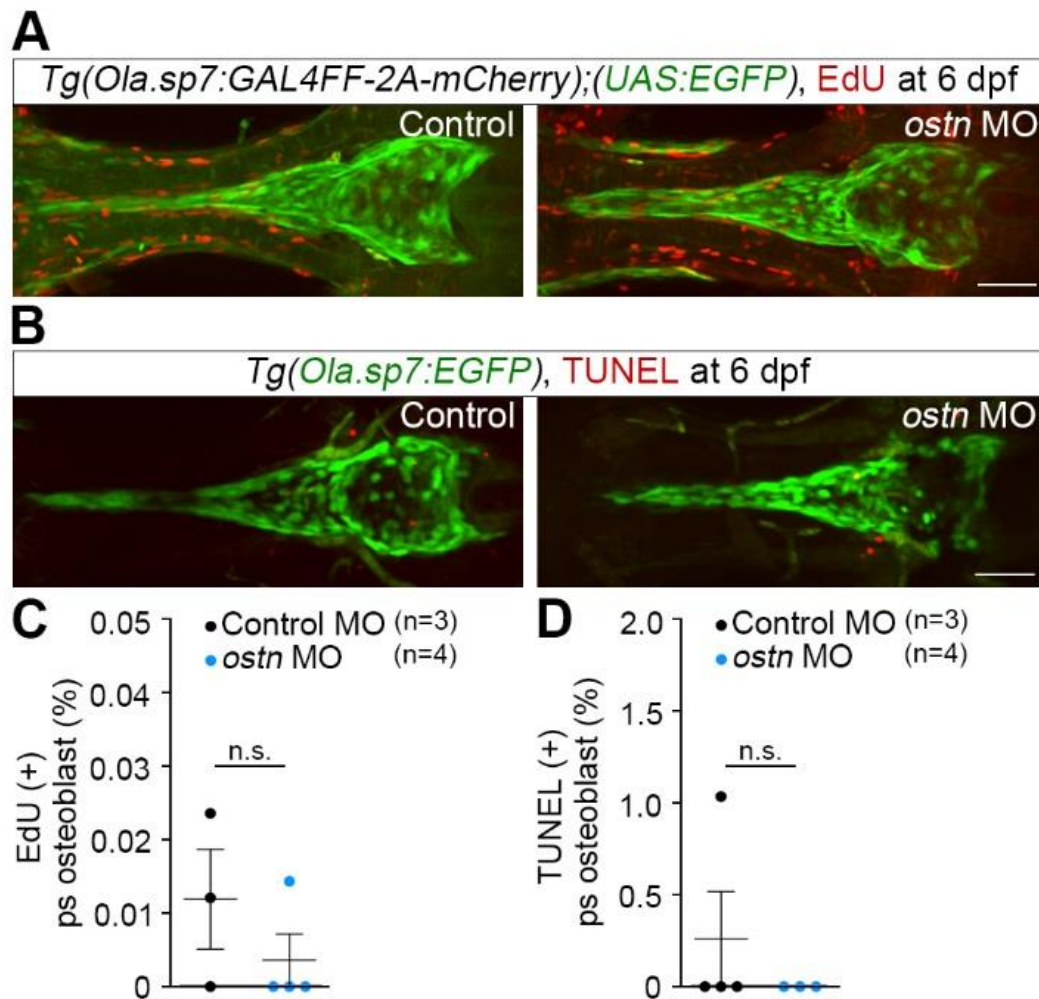


**Fig. S7. Osteoblast proliferation and apoptosis were comparable between the *ostn* mutant and control larvae.** (A) Representative confocal images of 5-ethynyl-2-deoxyuridine (EdU) incorporation (red) in the ps of the *Tg(Ola.sp7:GAL4FF-2A-mCherry);(UAS:EGFP)* larvae at 6 dpf injected with control MO (left panel) and *ostn* MO (right panel). EdU-positive cells are marked by red. (B) Representative confocal images of TdT-mediated dUTP nick end labeling (TUNEL) staining (red) in the ps of the *Tg(Ola.sp7:EGFP)* larvae at 6 dpf injected with control MO (left panel) and *ostn* MO (right panel). (C) Quantitative analyses of EdU-positive percentage of EGFP-positive osteoblasts in the ps. (D) Quantitative analyses of (B). The data were analyzed by Student's *t*-test. n.s., no significance between two groups. Error bars indicate s.e.m. Scale bars, 50  $\mu$ m.

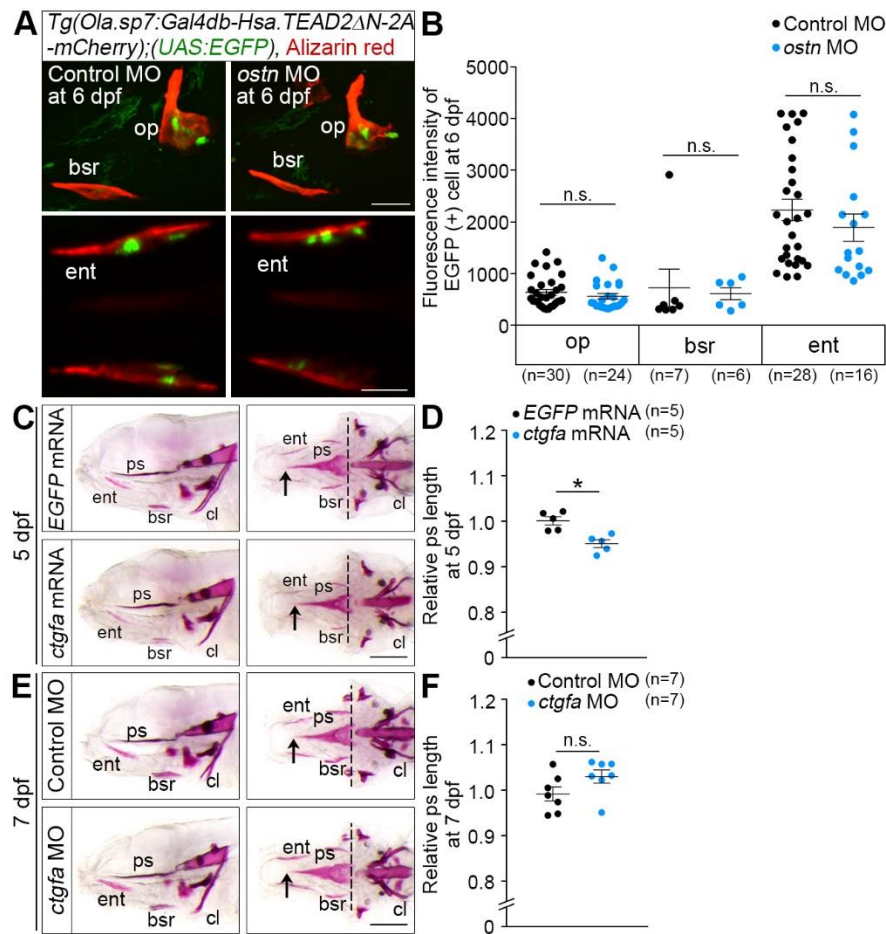


**Fig. S8. *Ctgfa* affects the ps formation.** (A) Representative confocal images of the op, bsr (upper panels), and ent (lower panels) of the *Tg(Ola.sp7:Gal4db-Hsa.TEAD2ΔN-2A-mCherry);(UAS:EGFP)* larvae injected with control MO (left panels) or *ostn* MO (right panels) and stained with alizarin red at 6 dpf. ent, entopterygoid; bsr, branchiostegal ray; op, opercle. (B) Quantitative analyses of (A). The intensity of EGFP-positive area in each bone was plotted. The number of EGFP-positive area was indicated at the bottom. (C) Representative images of alizarin red staining of the 5 dpf larvae injected with *egfp* mRNA (upper panels) and *ctgfa* mRNA (lower panels). Lateral view (left panels) and ventral view (right panels), anterior to the left. Arrows and broken lines indicate the tip and the top of the concave in the caudal part of the ps, respectively. ps, parasphenoid; cl, cleithrum. (D) Quantitative analyses of (C). The length of the ps was measured similarly to Fig. 3E. (E) Representative images of alizarin red staining of the 7 dpf larvae injected with control MO (upper panels) and *ctgfa* MO (lower panels). Lateral view (left panels) and ventral view (right panels), anterior to the left. (F) Quantitative analyses of (E). The data were analyzed by Student's *t*-test. Statistical significance, \**p* < 0.05. n.s., no significance between two groups. Error bars indicate s.e.m. Scale bars, 50 μm (A) and 200 μm (C and E).

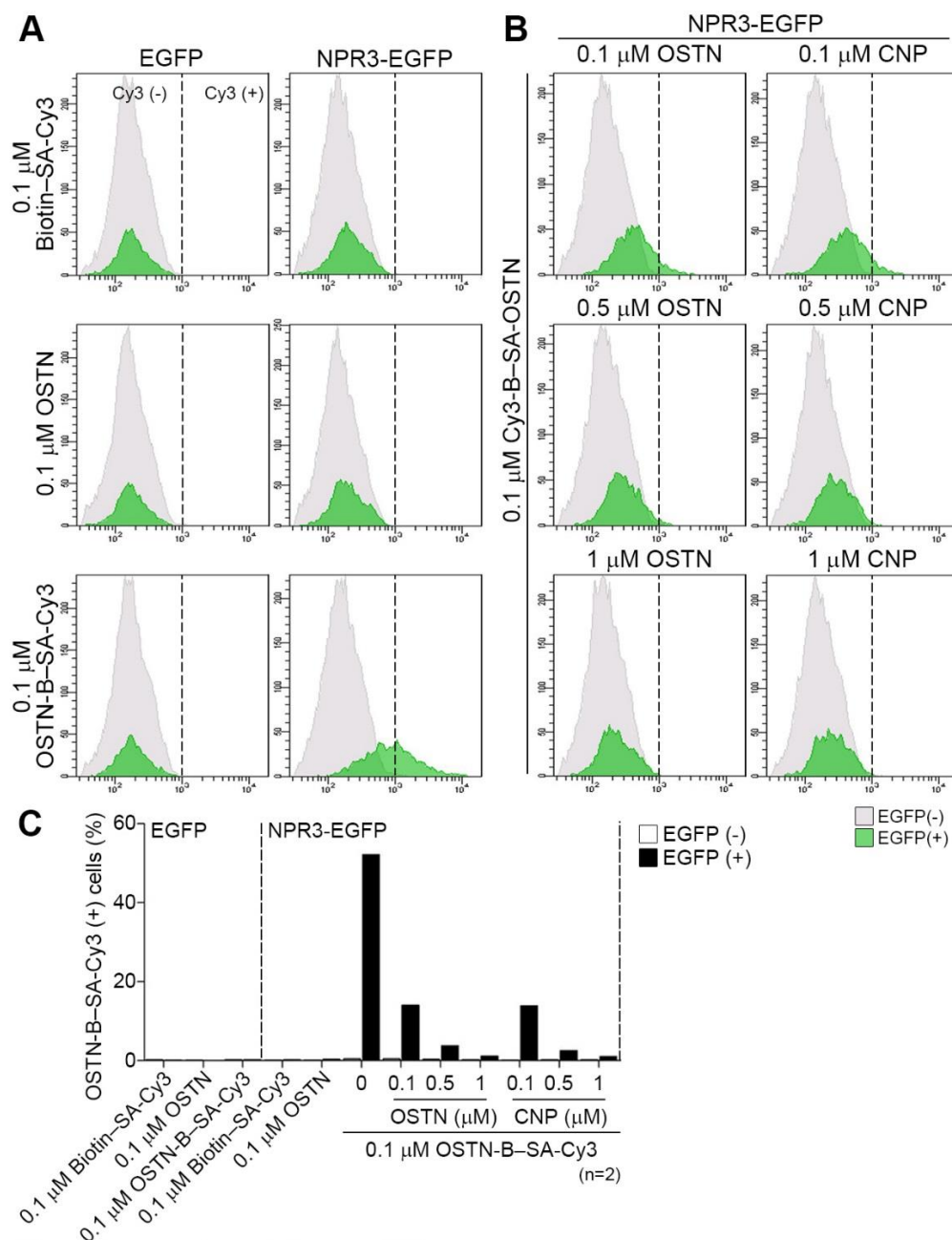


**Fig. S9. OSTN and CNP competitively bind to NPR3.** (A) Binding of biotin (top panels), unlabeled rat OSTN (middle panels), or biotin-labeled rat OSTN (OSTN-B) (bottom panels) to EGFP (left panels) or NPR3-EGFP (right panels) overexpressed in HEK293T cells was analyzed by flow cytometry. Binding of OSTN-B was detected by Cy3-conjugated streptavidin (SA-Cy3). (B) Binding of OSTN-B to NPR3-EGFP overexpressed in HEK293T cells in the presence of unlabeled rat OSTN (right panels) or human CNP (left panels) at the dose indicated on the top was analyzed similarly to (A). Note that binding of OSTN-B to NPR3-EGFP was inhibited by either unlabeled rat OSTN or human CNP. (C) Quantitative analyses of (A) and (B).



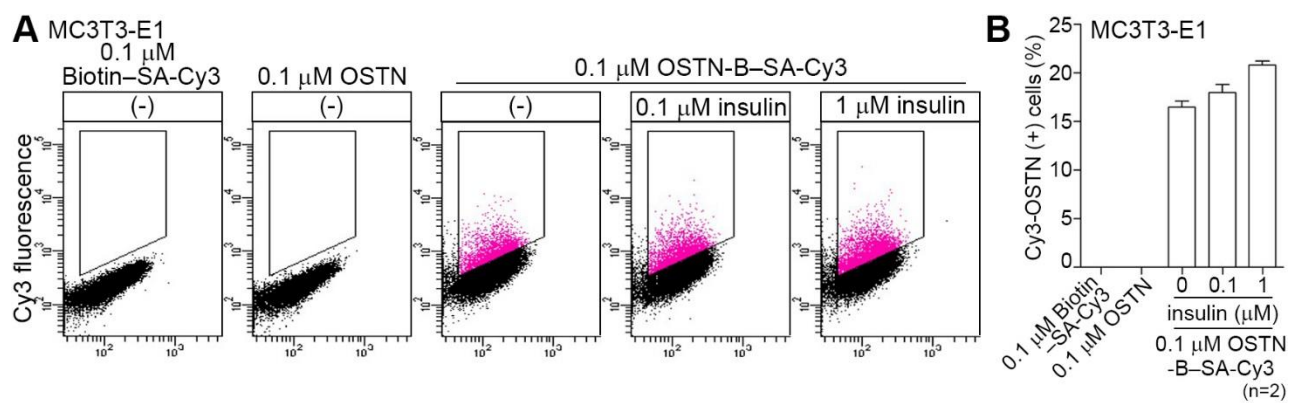


**Fig. S10. Binding of OSTN to NPR3 is not affected by insulin. (A)**

Competitive binding of biotin-labeled rat OSTN with insulin to MC3T3-E1 cells was analyzed by flow cytometry. The binding of OSTN-B in the presence of insulin indicated at the top to MC3T3-E1 cells was shown as a dot-plot data. **(B)** Quantitative analyses of (A). Error bars indicate s.e.m.

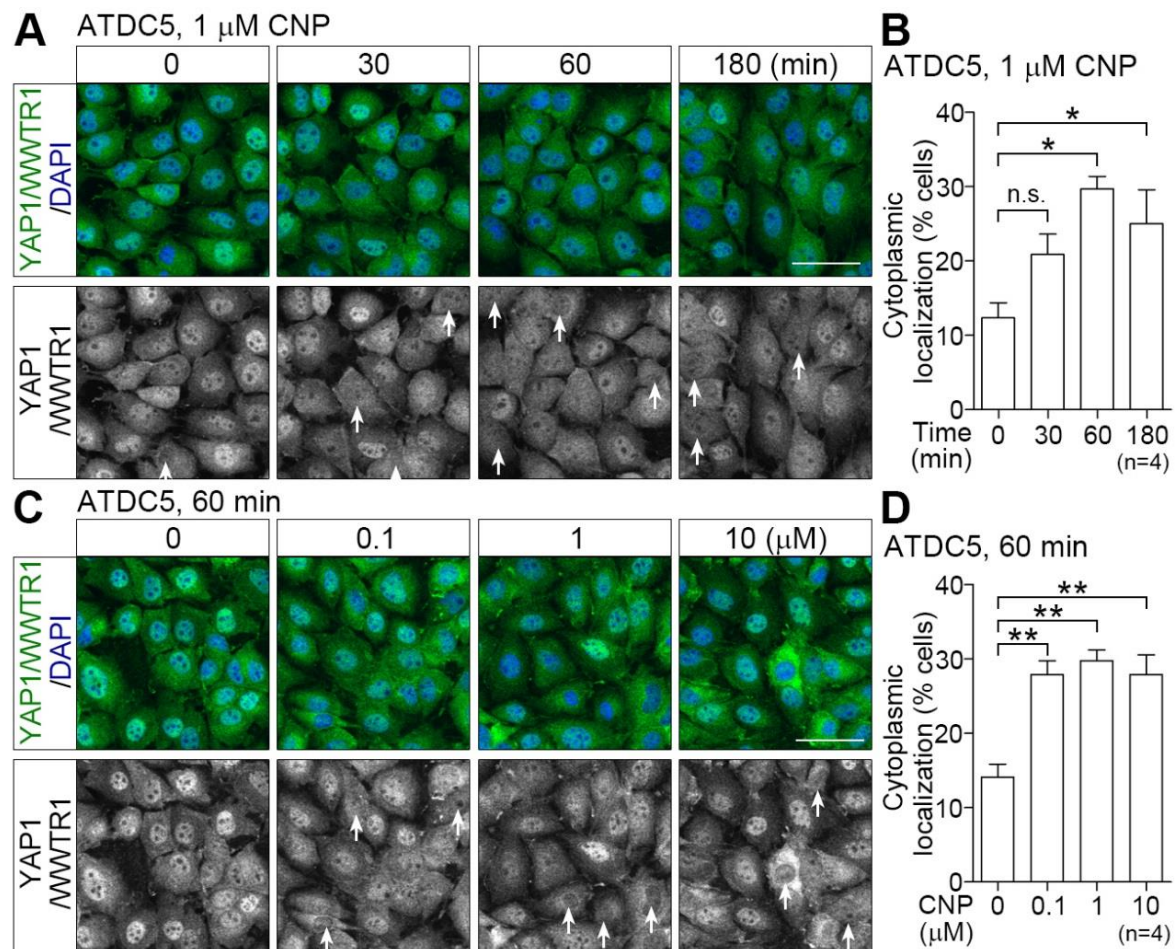


**Fig. S11. CNP induces nuclear export of YAP1/WWTR1 in ATDC5 cells.** (A) Representative images of immunostaining of ATDC5 cells stimulated with 1  $\mu$ M CNP for the time indicated at the top with anti-YAP1/WWTR1 antibody and DAPI. Double staining of DAPI (blue) and YAP1/ WWTR1 (green) (upper panels) and YAP1/WWTR1 staining displayed in gray-scale image (lower panels). Arrows indicate the cells exhibiting nuclear export of YAP1/WWTR1. (B) Quantitative analyses of nuclear export of YAP1/WWTR1 in (A) were analyzed similarly to Fig. 6D. (C) Representative images of immunostaining of ATDC5 cells stimulated for 60 min with CNP at the dose indicated at the top with anti-YAP1/WWTR1 antibody and DAPI. (D) Quantitative analyses of nuclear export of YAP1/WWTR1 in (D) were analyzed similarly to Fig. 6D. The data were analyzed by one-way ANOVA with Turkey's test. Statistical significance, \* $p < 0.05$ ; \*\* $p < 0.01$ . n.s., no significance between two groups. Error bars indicate s.e.m. Scale bars, 50  $\mu$ m.

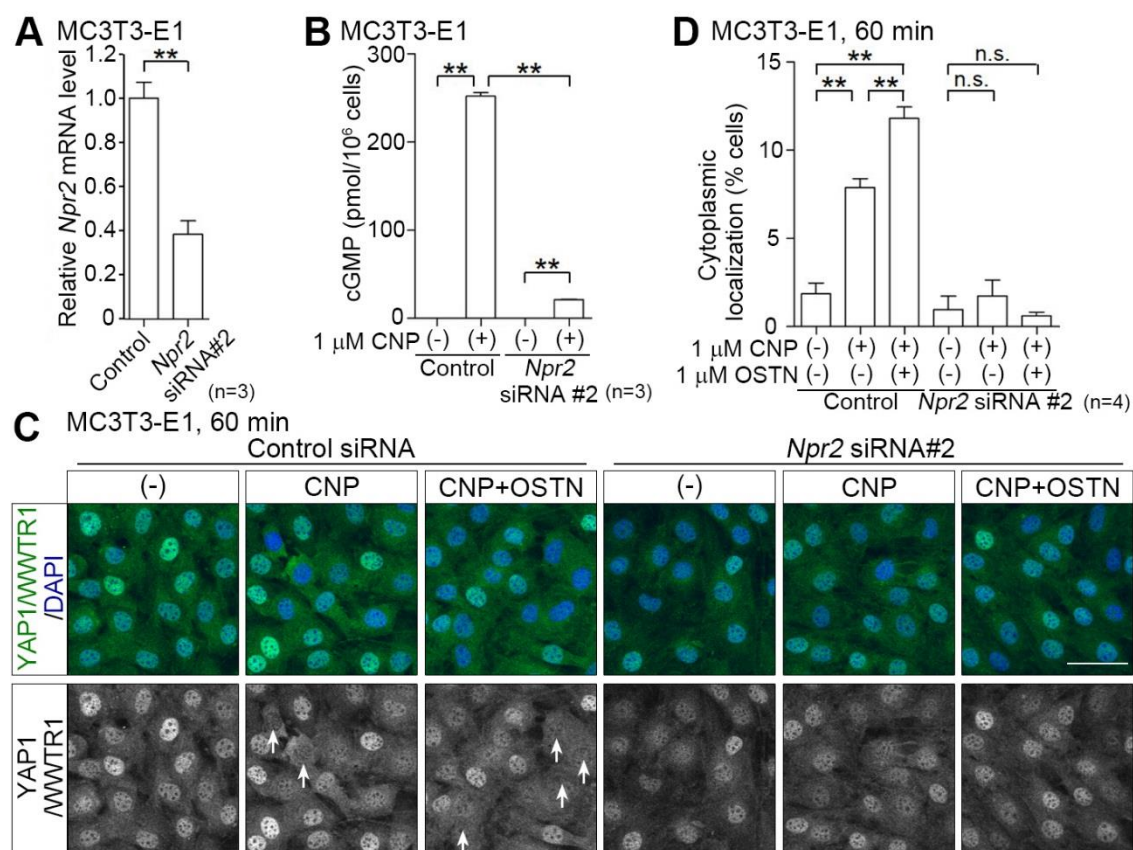


**Fig. S12. *Npr2* siRNA#2 pretreatment reduces CNP-induced nuclear export of YAP1/WWTR1.** (A) qRT-PCR analyses of *Npr2* mRNA of MC3T3-E1 cells treated with siRNA against *Npr2* for 72 h to validate the knockdown efficiency of siRNAs. (B) Measurement of cGMP in MC3T3E1 cells pretreated with siRNAs for 72 h and stimulated with 1  $\mu$ M CNP for 15 min as indicated at the bottom. (C) Representative images of Immunostaining of MC3T3-E1 cells pretreated with either control siRNA (left three panels) or *Npr2* siRNA#2 (right three panels) and simulated with peptide (1  $\mu$ M CNP and/or 1  $\mu$ M OSTN) as indicated at the top with anti-YAP1/WWTR1 antibody. (D) Quantitative analyses of the nuclear exports of YAP1/WWTR1 of the cells in (C) were analyzed similarly to Fig. 6D. The data were analyzed by Student's *t*-test or one-way ANOVA with Turkey's test. Statistical significance, \*\*  $p < 0.01$ . n.s., no significance between two groups. Error bars indicate s.e.m. Scale bar, 50  $\mu$ m.

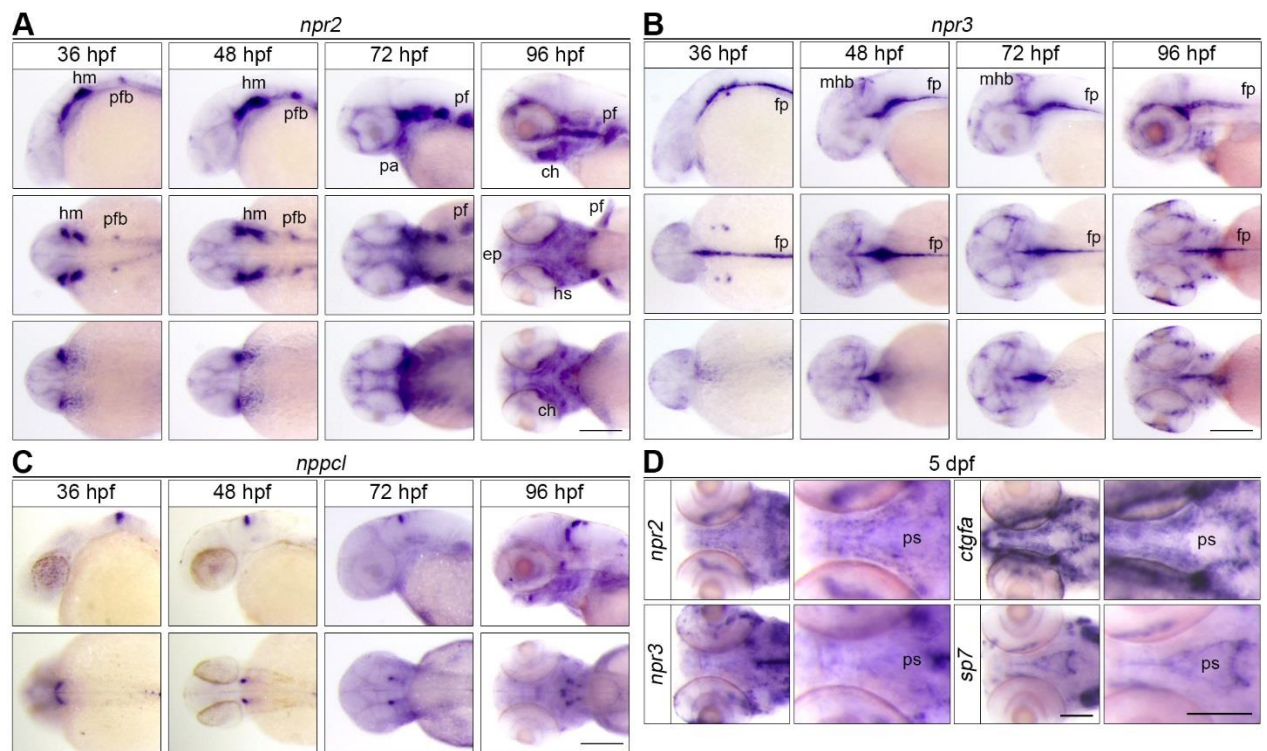


**Fig. S13. The expression of *npr2*, *npr3* and *nppcl* mRNAs.** (A-B) WISH analyses of *npr2* (A) and *npr3* (B) mRNAs of the larvae at the time point indicated at the top. Lateral view (upper panels), dorsal view (middle panels), and ventral view (left panels), anterior to the left. hm, head mesenchyme; pfb, pectoral fin bud; pa, pharyngeal arches; pf, pectoral fin; ch, ceratohyal; ep, ethmoid plate; fp, floor plate; mhb, midbrain hind brain boundary. (C) WISH analyses of *nppcl* mRNA of the larvae at the time point indicated at the top. Lateral view (upper panels), dorsal view (lower panels), anterior to the left. (D) WISH analyses of mRNAs indicated at the left of the ps area in the 5 dpf larvae resected the lower jaw. Ventral view of the head (left panels) and high magnification image (right panels), anterior to the left. *sp7* mRNA expression is a positive control to show the ps. Scale bars, 200  $\mu$ m.



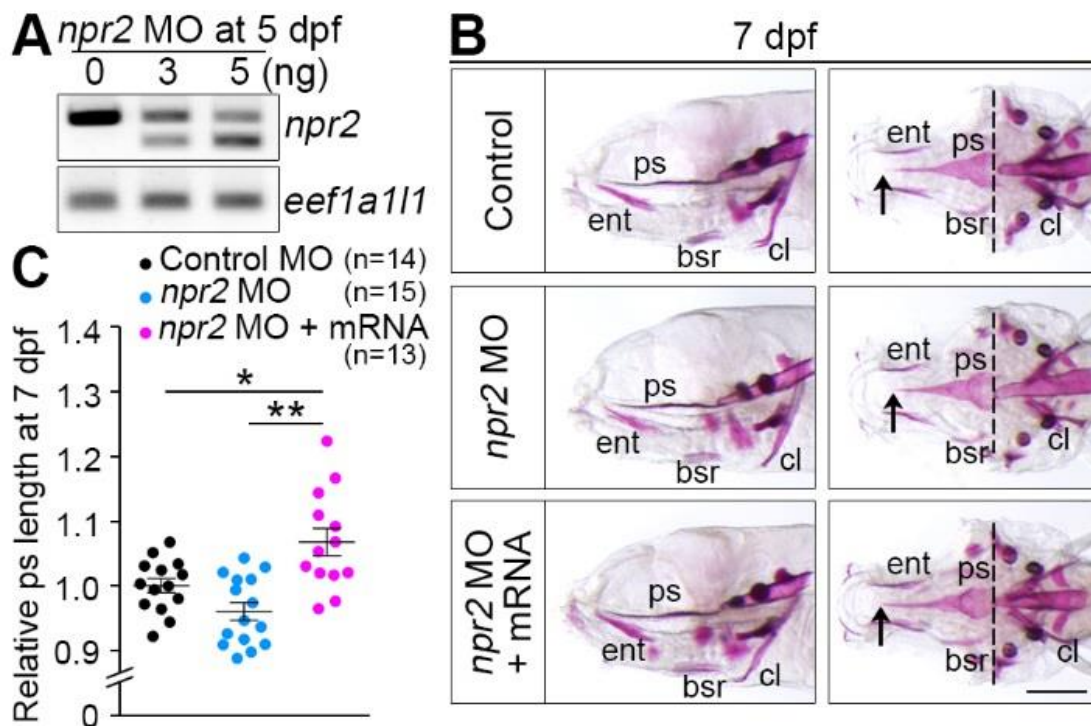


**Fig. S14. Validation of the *npr2* MO.** (A) Representative RT-PCR analyses of *npr2* (upper panel) and *eef1a1l1* (lower panel) mRNAs of the 5 dpf larvae injected with vehicle (left), 3 ng *npr2* MO (center), and 5 ng *npr2* MO (right). MO injection resulted in shorter PCR products. (B) Representative images of alizarin red staining of the 7 dpf larvae injected with control MO (top), 5 ng *npr2* MO (middle), and 5 ng *npr2* MO with 160 pg *npr2*-EGFP mRNA (bottom). Lateral view (left panels) and ventral view (right panels), anterior to the left. ent, entopterygoid; ps, parasphenoid; bsr, branchiostegal ray; cl, cleithrum. (C) Quantitative analyses of (B). The length of the ps was measured similarly to Fig. 3E. The data were analyzed by one-way ANOVA with Turkey's test. Statistical significance, \* $p < 0.05$ ; \*\* $p < 0.01$ . Error bars indicate s.e.m. Scale bar, 200  $\mu$ m.

## References

- Asakawa,K., Suster,M.L., Mizusawa,K., Nagayoshi,S., Kotani,T., Urasaki,A., Kishimoto,Y., Hibi,M., and Kawakami,K.** (2008). Genetic dissection of neural circuits by Tol2 transposon-mediated Gal4 gene and enhancer trapping in zebrafish. *Proc. Natl. Acad. Sci. U. S. A* **105**, 1255-1260.
- Cermak,T., Doyle,E.L., Christian,M., Wang,L., Zhang,Y., Schmidt,C., Baller,J.A., Somia,N.V., Bogdanove,A.J., and Voytas,D.F.** (2011). Efficient design and assembly of custom TALEN and other TAL effector-based constructs for DNA targeting. *Nucleic Acids Res.* **39**, e82.
- Distel,M., Wullimann,M.F., and Koster,R.W.** (2009). Optimized Gal4 genetics for permanent gene expression mapping in zebrafish. *Proc. Natl. Acad. Sci. U. S. A* **106**, 13365-13370.
- Doyle,E.L., Booher,N.J., Standage,D.S., Voytas,D.F., Brendel,V.P., Vandyk,J.K., and Bogdanove,A.J.** (2012). TAL Effector-Nucleotide Targeter (TALE-NT) 2.0: tools for TAL effector design and target prediction. *Nucleic Acids Res.* **40**, W117-W122.
- Fukui,H., Terai,K., Nakajima,H., Chiba,A., Fukuhara,S., and Mochizuki,N.** (2014). S1P-Yap1 signaling regulates endoderm formation required for cardiac precursor cell migration in zebrafish. *Dev. Cell* **31**, 128-136.
- Halloran,M.C., Sato-Maeda,M., Warren,J.T., Su,F., Lele,Z., Krone,P.H., Kuwada,J.Y., and Shoji,W.** (2000). Laser-induced gene expression in specific cells of transgenic zebrafish. *Development* **127**, 1953-1960.
- Kashiwada,T., Fukuhara,S., Terai,K., Tanaka,T., Wakayama,Y., Ando,K., Nakajima,H., Fukui,H., Yuge,S., Saito,Y. et al.** (2015). beta-catenin-dependent transcription is central to Bmp-mediated formation of venous vessels. *Development* **142**, 497-509.
- Kawakami,K., Takeda,H., Kawakami,N., Kobayashi,M., Matsuda,N., and Mishina,M.** (2004). A transposon-mediated gene trap approach identifies developmentally regulated genes in zebrafish. *Dev. Cell* **7**, 133-144.
- Kimmel,C.B., Ballard,W.W., Kimmel,S.R., Ullmann,B., and Schilling,T.F.** (1995). Stages of embryonic development of the zebrafish. *Dev. Dyn.* **203**, 253-310.
- Knopf,F., Hammond,C., Chekuru,A., Kurth,T., Hans,S., Weber,C.W., Mahatma,G., Fisher,S., Brand,M., Schulte-Merker,S. et al.** (2011). Bone

regenerates via dedifferentiation of osteoblasts in the zebrafish fin. *Dev. Cell* **20**, 713-724.

**Kurita,R., Sagara,H., Aoki,Y., Link,B.A., Arai,K., and Watanabe,S.** (2003). Suppression of lens growth by alphaA-crystallin promoter-driven expression of diphtheria toxin results in disruption of retinal cell organization in zebrafish. *Dev. Biol.* **255**, 113-127.

**Spoorendonk,K.M., Peterson-Maduro,J., Renn,J., Trowe,T., Kranenbarg,S., Winkler,C., and Schulte-Merker,S.** (2008). Retinoic acid and Cyp26b1 are critical regulators of osteogenesis in the axial skeleton. *Development* **135**, 3765-3774.

**Uemura,M., Nagasawa,A., and Terai,K.** (2016). Yap/Taz transcriptional activity in endothelial cells promotes intramembranous ossification via the BMP pathway. *Sci. Rep.* **6**, 27473.

**Urasaki,A., Morvan,G., and Kawakami,K.** (2006). Functional dissection of the Tol2 transposable element identified the minimal cis-sequence and a highly repetitive sequence in the subterminal region essential for transposition. *Genetics* **174**, 639-649.



**Supplementary movie 1.** Video image of a beating heart of *Tg(myl7:NLS-mCherry)* larva at 72 hpf obtained by a light sheet microscope.

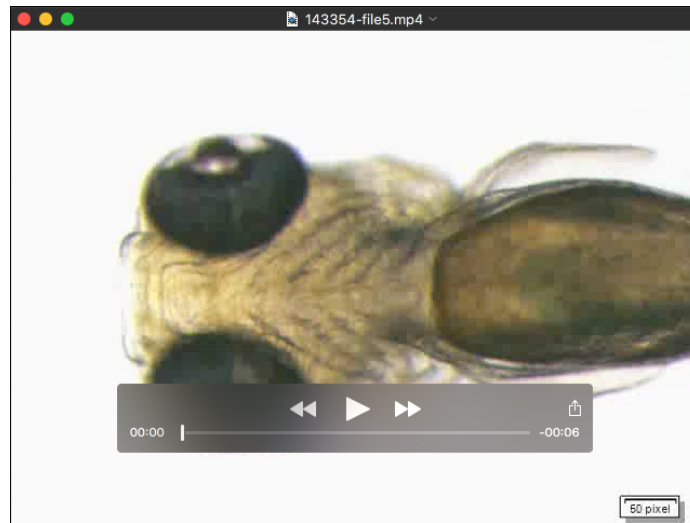




**Supplementary movie 2.** Video image of a beating heart of *Tg(myl7:actn2-tdEos)* larva at 72 hpf obtained by a light sheet microscope.



**Supplementary movie 3.** Video image of a beating heart of larva injected with control MO at 5 dpf obtained by a stereo microscope. Ventral view, anterior to the left. Scale bar, 125  $\mu\text{m}$ .



**Supplementary movie 4.** Video image of a beating heart of larva injected with *ostn* MO at 5 dpf obtained by a stereo microscope. Ventral view, anterior to the left. Scale bar, 125  $\mu$ m.